Author Manuscript

Author Manuscript

Author Manuscript

Author Manuscript

HHS Public Access

Author manuscript

Nat Cell Biol. Author manuscript; available in PMC 2016 May 01.

Published in final edited form as:

Nat Cell Biol. 2015 November ; 17(11): 1484–1496. doi:10.1038/ncb3255.

6-phosphogluconate dehydrogenase links oxidative PPP, lipogenesis and tumor growth by inhibiting LKB1-AMPK signaling

Ruiting Lin[1,14], **Shannon Elf**[1,14], **Changliang Shan**[1,14], **Hee-Bum Kang**[1], **Quanjiang Ji**[6], **Lu Zhou**[6], **Taro Hitosugi**[1], **Liang Zhang**[6], **Shuai Zhang**[4], **Jae Ho Seo**[1], **Jianxin Xie**[7], **Meghan Tucker**[7], **Ting-Lei Gu**[7], **Jessica Sudderth**[8], **Lei Jiang**[8], **Matthew Mitsche**[9], **Ralph J. DeBerardinis**[8], **Shaoxiong Wu**[2], **Yuancheng Li**[3], **Hui Mao**[3], **Peng R. Chen**[10], **Dongsheng Wang**[1], **Georgia Zhuo Chen**[1], **Selwyn J. Hurwitz**[5], **Sagar Lonial**[1], **Hanna J. Khoury**[1], **Martha L. Arellano**[1], **Hanna J. Khoury**[1], **Fadlo R. Khuri**[1], **Benjamin H. Lee**[11], **Qunying Lei**[12], **Daniel J. Brat**[4], **Keqiang Ye**[4], **Titus J. Boggon**[13], **Chuan He**[6], **Sumin Kang**[1,15], **Jun Fan**[1,15], and **Jing Chen**[1,15]

[1]Department of Hematology and Medical Oncology, Winship Cancer Institute of Emory, Emory University School of Medicine, Atlanta, Georgia 30322, USA

[2]Department of Chemistry, Emory University School of Medicine, Atlanta, Georgia 30322, USA

[3]Department of Radiology, Emory University School of Medicine, Atlanta, Georgia 30322, USA

[4]Department of Pathology and Laboratory Medicine, Emory University School of Medicine, Atlanta, Georgia 30322, USA

[5]Department of Pediatrics, Emory University School of Medicine, Atlanta, Georgia 30322, USA

[6]Department of Chemistry and Institute for Biophysical Dynamics, University of Chicago, Chicago, Illinois 60637, USA

[7]Cell Signaling Technology, Inc. (CST), Danvers, Massachusetts 01923, USA

[8]Children's Research Institute, Dallas, Texas 75390, USA

[9]Eugene McDermott Center for Human Growth and Development UT Southwestern Medical Center, Dallas, Texas 75390, USA

Users may view, print, copy, and download text and data-mine the content in such documents, for the purposes of academic research, subject always to the full Conditions of use:http://www.nature.com/authors/editorial_policies/license.html#terms

[15]Correspondence should be addressed to S.K., J.F. or J.C. (smkang@emory.edu, jfan3@emory.edu, or jchen@emory.edu).

[14]These authors contributed equally to this work.

AUTHOR CONTRIBUTIONS

R.L., S.E. and C.S. contributed equally to this work. J.X., T.-L.G., S.Z., K.Y., P.C., D.J.B., M.L.A., S.L., H.J.K.,Q.L. and F.R.K. provided critical reagents. S.J.H. performed data analysis of pharmacokinetics studies. M.T. and T.-L.G. performed mass spectrometry based assays. Q.J., L. Zhou, L. Zhang and C.H. performed biochemical analysis of lysine-acetylated 6PGD and molecular docking studies and analyzed the data. J.S., L.J., M.M., R.J.D., S.W., Y.L. and H.M. performed quantitative mass spectrometry and NMR based assays, and analyzed data. B.H.L. performed the histopathological analyses. T.J.B. performed structural analyses. D.W. and G.Z.C. helped with xenograft experiments. C.S., S.E., H.-B.K., J.-H.S. T.H., and J.F. performed all other experiments. R.L., S.E. C.S., S.K., J.F. and J.C. designed the study and wrote the paper. S.K., J.F. and J.C. are senior authors and jointly managed the project. All authors read and approved the final manuscript.

COMPETING FINANCIAL INTERESTS

The authors declare no competing financial interests.

Author Manuscript Author Manuscript Author Manuscript Author Manuscript

[10]College of Chemistry and Molecular Engineering Peking University, Beijing, China 100871

[11]Novartis Institutes for BioMedical Research, Cambridge, Massachusetts 02139, USA

[12]School of Basic Medical Sciences, Fudan University, Shanghai 200032, China.

[13]Department of Pharmacology, Yale University School of Medicine, New Haven, Connecticut 06520, USA.

Abstract

The oxidative pentose phosphate pathway (PPP) contributes to tumor growth, but the precise contribution of 6-phosphogluconate dehydrogenase (6PGD), the third enzyme in this pathway, to tumorigenesis remains unclear. We found that suppression of 6PGD decreased lipogenesis and RNA biosynthesis and elevated ROS levels in cancer cells, attenuating cell proliferation and tumor growth. 6PGD-mediated production of ribulose-5-phosphate (Ru-5-P) inhibits AMPK activation by disrupting the active LKB1 complex, thereby activating acetyl-CoA carboxylase 1 and lipogenesis. Ru-5-P and NADPH are thought to be precursors in RNA biosynthesis and lipogenesis, respectively; thus, our findings provide an additional link between oxidative PPP and lipogenesis through Ru-5-P-dependent inhibition of LKB1-AMPK signaling. Moreover, we identified and developed 6PGD inhibitors, Physcion and its derivative S3, that effectively inhibited 6PGD, cancer cell proliferation and tumor growth in nude mice xenografts without obvious toxicity, suggesting that 6PGD could be an anticancer target.

The Warburg effect in cancer cells describes increased aerobic glycolysis, producing not only ATP but also precursors for anabolic biosynthesis of macromolecules that are necessary for cell proliferation and rapidly tumor growth [1-3]. Glycolytic intermediate glucose-6-phosphate is diverted into the oxidative pentose phosphate pathway (PPP), which produces ribose-5-phosphate (R-5-P) that is precursor for nucleotide synthesis [3-8]. Oxidative PPP also produces nicotinamide adenine dinucleotide phosphate (NADPH), which is not only required by biosynthesis of lipids but also a crucial antioxidant that quenches the reactive oxygen species (ROS) produced during rapid proliferation of cancer cells and maintains redox homeostasis [2]. Therefore, oxidative PPP plays a crucial role in metabolic coordination of glycolysis, biosynthesis and appropriate redox status to provide an overall metabolic advantage to tumor cell proliferation and disease development. Indeed, inhibition of glucose-6-phosphate dehydrogenase (G6PD), the first enzyme of the oxidative PPP that produces NADPH, results in attenuated cell growth with potentiated H_2O_2-mediated cell death, probably due to lack of NADPH [9-12]. Moreover, matrix-detachment upregulates G6PD, which confers anoikis-resistance to detached ErbB2 transformed MCF-10A breast cancer cells [13]. Furthermore, 6-amino-nicotinamide (6-AN), an inhibitor of G6PD, has demonstrated anti-tumorigenic effects in leukemia, glioblastoma and lung cancer cells [14].

6PGD is the third enzyme in the oxidative PPP, which converts 6-phosphogluconate (6-PG) to Ru-5-P and produces NADPH. We recently reported that glycolytic enzyme phosphoglycerate mutase 1 (PGAM1) signals through 6PGD to coordinate glycolysis and oxidative PPP in cancer cells, suggesting an important role for 6PGD in cancer cell metabolism and tumor growth [5]. However, although 6PGD has been reported to be

Author Manuscript Author Manuscript Author Manuscript Author Manuscript

upregulated in many cancers, including colorectal cancers [15], cervical intraepithelial neoplasia [16, 17], thyroid tumors [18] and lung cancers [19], it remains unclear whether and how 6PGD contributes to oxidative PPP flux and subsequent biosynthesis and redox homeostasis in cancer cells, as well as cancer cell proliferation and tumor growth. Sukhatme and Chan recently reported that knockdown of 6PGD in lung cancer H1975 cells resulted in attenuated cell proliferation and tumor size in xenograft mice. However, suppression of 6PGD in these cells did not cause defects in the oxidative PPP, nor affected intracellular levels of NADPH. Instead, 6PGD knockdown inhibited H1975 cell proliferation through induction of senescence [19, 20]. Thus, it remains important to determine whether 6PGD is commonly important for the oxidative PPP flux and related metabolic and proliferative properties in cancer cells.

The tumor suppressor liver kinase B1 (LKB1) is a crucial upstream kinase of adenine monophosphate-activated protein kinase (AMPK), and LKB1-AMPK signaling plays a central role in regulation of cell metabolism, survial and proliferation in response to nutrient and energy levels [21-23]. In particular, AMPK governs lipid metabolism by inhibiting fatty acid and cholesterol synthesis through direct phosphorylation of the metabolic enzymes acetyl-CoA carboxylase (ACC) 1 and 2 [23-25]. In addition, AMPK-dependent inhibition of ACC1 and ACC2 contributes to regulation of NADPH homeostasis by decreasing NADPH consumption in fatty-acid synthesis, which promotes tumor cell survival during energy stress [26, 27]. In this paper, we report that 6PGD activation is important for the oxidative PPP flux and tumor growth in diverse cancer cells, and thus represents a promising anti-cancer target. We present a molecular mechanism that explains how 6PGD regulates lipogenesis by controlling intracellular concentrations of its product Ru-5-P to inhibit LKB1-AMPK signaling, providing additional crosstalk between metabolic pathways and cell signaling networks.

RESULTS

6PGD is important for oxidative PPP and lipogenesis, as well as proliferative and tumor growth potential of cancer cells

We found that stable knockdown of 6PGD resulted in decreased cell proliferation with reduced 6PGD activity in a group of human tumor and leukemia cells, including human lung cancer H1299, H157 and H322, leukemia K562 and head and neck cancer 212LN cells, but not the control normal proliferating keratinocyte HaCaT cells (Figs. 1a-1b). Moreover, in a xenograft experiment in which nude mice were injected with control H1299 cells and 6PGD knockdown cells on the left and right flanks, respectively, the growth rate (Fig. 1c) and masses (Fig. 1d) of tumors derived from 6PGD knockdown cells were significantly reduced with decreased expression of cell proliferation marker Ki-67 assessed by immunohistochemical (IHC) staining (Fig. 1e) compared to those of tumors formed by control cells over a ~6-week time period. In addition, H1299 cells harboring an inducible 6PGD shRNA construct showed decreased 6PGD expression and activity (Fig. 1f), reduced cell proliferation (Fig. 1g) and attenuated tumor growth in xenograft mice (Fig. 1h-1j) in the presence of doxycycline, compared to cells without treatment. Similar results were obtained in K562 leukemia cells with stable 6PGD knockdown cells (Supplementary Figs. 1a-1b), or

Author Manuscript Author Manuscript Author Manuscript Author Manuscript

K562 cells harboring an inducible 6PGD shRNA construct in the presence and absence of doxycycline (Supplementary Figs. 1c-1g).

6PGD knockdown in H1299 cells also resulted in reduced oxidative PPP flux, NADPH/$NADP^+$ ratio and intracellular levels of Ru-5-P (6PGD product) but increased 6-PG (6PGD substrate) (Fig. 2a), as well as subsequently decreased intracellular levels of ribose-5-phosphate (R-5-P) and RNA biosynthesis (Fig. 2b). Similar results were obtained using additional cancer cell lines (Supplementary Fig. 1h-1k). The decreased R-5-P levels may be predominantly due to defected oxidative PPP in 6PGD KD cells, because the protein expression and enzyme activity levels of transketolase (TKT) in non-oxidative PPP (Fig. 2c, *left*) and sensitivity to TKT inhibitor oxythiamine (OT) in terms of R-5-P levels (Fig. 2c, *right*) were not altered in these cells. We also observed increased glycolytic rate (Fig. 2d) and lactate production (Fig. 2e) with elevated glucose uptake rate (Fig. 2f) and intracellular ATP levels (Fig. 2g) in distinct human cancer cells with 6PGD knockdown, whereas O_2 consumption rate in either the presence or absence of ATP synthase inhibitor oligomycin was not altered (Fig. 2i). Such increased glycolysis was likely due to 6-PG dependent activation of glycolytic enzyme phosphofructokinase (PFK) [28], as 6-PG activated PFK in a dose dependent manner (Fig. 2j) and 6PGD knockdown increased activity of PFK, but not other glycolytic enzymes in cells (Fig. 2k). These results demonstrate an important role of 6PGD in regulation and coordination between oxidative PPP and glycolysis in cancer cells and subsequent tumor growth, suggesting 6PGD as a promising anti-cancer target.

6PGD promotes lipogenesis by controlling intracellular Ru-5-P levels to inhibit AMPK

Interestingly, we observed decreased lipogenesis in cells with stable 6PGD knockdown (Fig. 3a) or induced 6PGD shRNA in the presence of doxycycline compared to control cells (Fig. 3b and Supplementary Fig. 2a). To test whether 6PGD regulates lipogenesis through its products Ru-5-P and NADPH, cell contents were obtained from parental or 6PGD knockdown H1299 cells after sonication, followed by incubation with increasing concentrations of Ru-5-P or NADPH to rescue the levels of Ru-5-P (~320 μM) or NADPH (7.2 μM) in 6PGD knockdown cells to be close to and exceed the physiological levels of Ru-5-P (~800 μM) or NADPH (9.0 μM) in control cells, respectively, prior to lipid biosynthesis assay. We found that restoration of Ru-5-P to physiological levels rescued not only the decreased intracellular R-5-P levels (Supplementary Fig. 2b) but also the reduced lipid biosynthesis (Fig. 3c, *upper*) in 6PGD knockdown cells, whereas rescue of NADPH to physiological levels did not affect the decreased lipogenesis in these cells, although amounts of NADPH exceeding physiological levels eventually resulted in increased lipogenesis (Fig. 3c, *lower*).

These data suggest that although NADPH serves as a precursor for lipid biosynthesis, the defect of lipogenesis in 6PGD knockdown cells is predominantly due to a Ru-5-P-dependent mechanism, which may affect a crucial step in lipogenesis. Indeed, we found that among the three key enzymes in the lipogenesis, acetyl-CoA carboxylase 1 (ACC1), but not ATP citrate lyase (ACLY) and fatty acid synthase (FASN), has decreased enzyme activity in 6PGD knockdown cells (Fig. 3d). AMPK inhibits ACC1 by phosphorylating Ser79, Ser1200, and Ser1215 [29-33]. Consistently, inhibition of AMPK by Compound C or shRNA

Author Manuscript Author Manuscript Author Manuscript Author Manuscript

(Supplementary Fig. 2c) also led to increased lipogenesis in 6PGD KD cells (Fig. 3e), suggesting that 6PGD may promote lipogenesis by controlling Ru-5-P to inhibit AMPK and subsequently activate ACC1.

Ru-5-P disrupts active LKB1 complex

Consistently, 6PGD knockdown resulted in increased activating T172 phosphorylation of AMPK [21] and inhibitory 79 phosphorylation of ACC1, while incubation with increasing concentrations of Ru-5-P (Fig. 4a, *left*), but not R-5-P (Fig. 4a, *right*) or NADPH (Supplementary Fig. 2d), reduced AMPK and ACC1 phosphorylation levels. Similar results were obtained using K562 cells with 6PGD knockdown (Supplementary Fig. 2e). However, incubation with Ru-5-P did not affect AMPK activity in an *in vitro* kinase assay using purified AMPK (Supplementary Fig. 2f), suggesting that Ru-5-P may inhibit an upstream activating kinase of AMPK, likely LKB1. Indeed, Ru-5-P inhibited the kinase activity of LKB1 wild type (WT) but not a kinase dead form (K78M) in a dose-dependent manner in an *in vitro* LKB1 kinase assay using purified LKB1 protein incubated with purified AMPK as an exogenous substrate (Fig. 4b, *left*). Similar results were obtained using purified active LKB1 incubated with purified AMPK (Fig. 4b, *upper right* and Supplementary Fig. 2g) or myelin basic protein (MBP) (Fig. 4b, *lower right*) as exogenous substrates. In contrast, incubation with increasing concentrations of R-5-P or NADPH did not affect LKB1 activity (Fig. 4b, *right* and Supplementary Fig. 2h, respectively).

LKB1 forms a complex with pseudokinase Ste20-related adaptor (STRAD) and scaffolding-like adaptor protein mouse protein 25 (MO25) to achieve full activation [33-36]. We found that treatment with increasing concentrations of Ru-5-P led to decreased association between LKB1, STRAD and MO25 in H1299 cell lysates (Supplementary Fig. 2i) without affecting the protein levels of LKB1, MO25 and STRAD (Supplementary Fig. 2j). Moreover, 6PGD knockdown resulted in increased binding among LKB1, STRAD and MO25, whereas rescue of decreased levels of Ru-5-P (Fig. 4c, *left*), but not R-5-P (Fig. 4c, *right*) or NADPH (Supplementary Fig. 2k), in 6PGD KD cell lysates reversed the increased formation of LKB1-STRAD-MO25 complex. Similar results were obtained using K562 cells (Supplementary Fig. 2l). Furthermore, treatment with Ru-5-P was sufficient to trigger the disruption of purified active LKB1 complex within 5 minutes (Fig. 4d), which eventually attenuated AMPK binding to LKB1 (Fig. 4e), whereas incubation with R-5-P or NADPH for 20 minutes had no effect (Supplementary Fig. 2m).

6PGD is important for coordination between biosynthesis and redox homeostasis to promote cancer cell proliferation

6PGD knockdown also resulted in increased ROS levels, which was consistent with decreased NADPH/$NADP^+$ ratio, while treatment with an antioxidant agent N-acetylcysteine (NAC) did not rescue reduced lipogenesis (Supplementary Fig. 3a) but significantly reduced ROS levels (Fig. 5a and Supplementary Fig. 3b). Although treatments with either Compound C or NAC or both (Supplementary Figs. 3c-3e), or knockdown of AMPK (Supplementary Fig. 3f) did not affect H1299 cell proliferation, such treatments in 6PGD knockdown cells significantly rescued the reduced cell proliferation (Supplementary Fig. 3g), and combined treatment with NAC and Compound C or AMPK shRNA

Author Manuscript Author Manuscript Author Manuscript Author Manuscript

demonstrated further rescue effect (Fig. 5b). Moreover, we found that knockdown of LKB1 abolished AMPK phosphorylation enhanced by 6PGD knockdown (Supplementary Fig. 3h), which, although did not affect the decreased Ru-5-P levels, reversed the reduced lipogenesis in 6PGD knockdown cells (Supplementary Fig. 3i).

Consistent with these findings, although stable knockdown of 6PGD in LKB1-deficient A549 cells resulted in decreased 6PGD activity and subsequent Ru-5-P levels (Figs. 5c-5d, respectively), 6PGD knockdown did not affect phosphorylation levels of AMPK and lipogenesis (Figs. 5e-5f, respectively). Additionally, rescue of the decreased Ru-5-P levels in cell lysates from A549 cells with 6PGD knockdown did not affect AMPK phosphorylation levels or lipogenesis (Figs. 5g-5h, respectively), whereas NAC treatment completely rescued decreased cell proliferation (Fig. 5i) by reversing increased ROS level (Fig. 5j) in A549 cells with stable 6PGD knockdown. Furthermore, expression of LKB1 WT but not the kinase-dead form K78M in LKB1-depicient A549 cells with 6PGD knockdown resulted in increased AMPK activation, decreased lipogenesis that was rescued by Ru-5-P treatment, and further decreased cell proliferation that was only partially rescued by NAC treatment, while expression of either LKB1 WT or K78M did not affect the decreased Ru-5-P levels in these cells (Supplementary Figs. 3j-3n, respectively).

Moreover, although knockdown of 6PGD in normal proliferating HaCaT cells also resulted in decreased 6PGD activity (Fig. 1b), Ru-5-P level and oxidative PPP flux along with increased AMPK phosphorylation and reduced lipogenesis (Fig. 5k-5n, respectively), 6PGD knockdown did not significantly affect cell proliferation of HaCaT cells (Fig. 1a), suggesting that the 6PGD-dependent regulation of LKB1-AMPK cascade and subsequent lipogenesis through Ru-5-P also exists in normal proliferating cells, but that these cells rely less on this regulatory mechanism for cell proliferation compared to cancer cells.

Discovery and Development of Physcion and its derivative S3 as 6PGD inhibitors

We next designed a screening strategy using an *in vitro* 6PGD assay (Fig. 6a). We identified Physcion ($C_{16}H_{12}O_5$; 1,8-Dihydroxy-3-methoxy-6-methyl-anthraquinone; Emodin-3-methyl ether) as a 6PGD inhibitor from a library of FDA approved 2,000 small molecule compounds (Fig. 6a), which effectively inhibits 6PGD but not G6PD (Fig. 6b). A Physcion derivative S3 ($C_{15}H_{10}O_4$; 1-Hydroxy-8-methoxy-anthraquinon; Fig. 6a) was identified with improved solubility from a group of 10 commercially available Physcion derivatives. Physcion and S3 inhibited 6PGD with absolute IC_{50} values of approximately 38.5 μM and 17.8 μM, respectively (Fig. 6c) and the Kd values of the Physcion-6PGD and S3-6PGD interaction were determined to be 26.0 μM and 17.1 μM, respectively, using a tryptophan fluorescence-based binding assay (Fig. 6d). Physcion did not effectively inhibit other $NADP^+$-dependent metabolic enzymes including G6PD, glutamate dehydrogenase 1 (GLUD1) and isocitrate dehydrogenase 1 (IDH1), nor glycolytic enzymes LDHA and PGAM1 (Fig. 6c). Moreover, Physcion inhibits 6PGD but not G6PD (Fig. 6e and Supplementary Fig. 4a), leading to a reduced proliferation of H1299 and K562 cells, whereas 6PGD knockdown cells were resistant to Physcion treatment (Fig. 6f and Supplementary Fig. 4b).

Author Manuscript Author Manuscript Author Manuscript Author Manuscript

Molecular docking study based on the crystal structure of 6PGD (PDB code: 3FWN) in complex with its substrate 6-PG suggests that Physcion fits in a pocket near the binding site of 6-PG surrounded by residues including M15, K76, K261 and H452 of 6PGD (Fig. 6g). Physcion forms hydrophobic interactions with these residues and a hydrogen bond with N103 via its 10-keto group (Fig. 6g). In support of this model, 6PGD M15A mutant showed resistance to Physcion or S3 treatment in an *in vitro* 6PGD enzyme activity assay (Fig. 6h and Supplementary Fig. 4c, respectively), and expression of M15A (Supplementary Fig. 4d) conferred Physcion- or S3-resistance to H1299 cells (Fig. 6i and Supplementary Fig. 4e, respectively), suggesting that 6PGD is a predominant target of Physcion and S3 in cancer cells.

Physcion and S3 inhibit cancer cell proliferation *in vitro* and tumor growth *in vivo*

Physcion treatment resulted in decreased cell viability of H1299, A549, 212LN and K562 cells in a dose dependent manner, but did not significantly affect the control proliferating cells including human dermal fibroblasts (HDF) and immortalized human melanocyte PIG1 cells (Fig. 6j). Physcion also inhibited cell proliferation of diverse human cancer cells including H1299, K562, MDA-MB-231 and 212LN cells (Fig. 6k and Supplementary Fig. 4f), and induced apoptosis in H1299 after 48 hours treatment, whereas knockdown of AMPK abolished induction of apoptosis upon Physcion treatment (Fig. 6l).

We found that Physcion treatment for 12 hours resulted in increased intracellular 6-PG levels but decreased Ru-5-P levels and NADPH/$NADP^+$ ratio, as well as reduced oxidative PPP flux and biosynthesis of RNA and lipids (Fig. 7a-7d, respectively), without induction of apoptosis (Supplementary Fig. 4g). Similar results were obtained using K562 cells treated with Physcion (Supplementary Figs. 4h-4l) and H1299 cells treated with S3 (Supplementary Figs. 5a-5b, respectively). Physcion or S3 also resulted in increased PFK activity in H1299 cells with increased lactate production and intracellular ATP levels (Supplementary Fig. 5c-5e, respectively), as well as increased phosphorylation levels of AMPK and ACC1 (Fig. 7e) and disruption of active LKB1 complex (Fig. 7f), while NAC treatment reversed the increased ROS levels in Physcion treated H1299 cells (Fig. 7g). Furthermore, NAC treatment (Fig. 7h and Supplementary Fig. 5f) or inhibition of AMPK by Compound C or shRNA (Fig. 7i) partially rescued the reduced cell proliferation of H1299 cells treated with 6PGD inhibitors. Similar results were obtained using K562 cells (Supplementary Figs. 5g-5j). Together these results were consistent with the phenomenon observed in 6PGD knockdown cells (Figs. 2-5).

Consistently, Physcion treatment decreased 6PGD activity and Ru-5-P levels in LKB1-deficient A549 cells (Figs. 7j-7k, respectively) but did not affect AMPK phosphorylation levels or lipogenesis (Figs. 7l-7m, respectively). Moreover, NAC treatment completely reversed the increased ROS level and rescued the decreased cell proliferation in Physcion-treated A549 cells (Figs. 7n-7o, respectively). Furthermore, normal proliferating HaCaT cells treated with Physcion showed decreased 6PGD activity and Ru-5-P level along with increased AMPK phosphorylation and reduced lipogenesis (Figs. 7p-7r, respectively) but unaltered cell proliferation (Fig. 7s). Similar results were obtained using normal proliferating HFF cells (Supplementary Figs. 5k-5o).

Author Manuscript Author Manuscript Author Manuscript Author Manuscript

S3 similarly inhibited cell viability of H1299 and K562 cells but not control proliferating PIG1 and HDF cells (Supplementary Fig. 6a). Chronic injection of S3 to nude mice for ~4 weeks revealed that 20 mg/kg/day administered intraperitoneally is a well-tolerated dose. In xenograft nude mice subcutaneously injected with H1299 cells, S3 treatment resulted in significantly decreased tumor growth and masses compared with mice receiving DMSO (Fig. 8a-8c) with decreased 6PGD activity (Fig. 8c, *right*) and reduced Ki-67 expression (Fig. 8d), suggesting that S3 inhibits 6PGD *in vivo* to confer a specific inhibitory effect on tumor cell proliferation. Similar results were obtained using K562 leukemia cell xenograft nude mice (Supplementary Fig. 6b-6e), and an orthotopic xenograft model of head and neck cancer, where human head and neck cancer Tu212 cells were orthotopically injected into the primary tumor site by submandibular injection to mylohypoid muscles of nude mice (Figs. 8e-8f; Supplementary Figs. 6f-6g). Additionally, chronic treatment with S3 to nude mice did not affect body weight, serum chemistry, or complete blood counts (CBC) and hematopoietic properties, nor cause notable differences in histopathological analyses (Supplementary Figs. 6h-6k, respectively) compared to the DMSO-treated group, suggesting that S3 treatment does not cause obvious toxicity *in vivo*.

6PGD represents a promising anti-leukemia target

Moreover, Physcion inhibited 6PGD in human primary leukemia cells (Fig. 8g, *left*), leading to decreased cell viability (Supplementary Fig. 7a), 6-PG accumulation and NADPH/$NADP^+$ ratio (Fig. 8h), increased phosphorylation levels of AMPK (Fig. 8i) and ACC1 (Fig. 8j), as well as increased lactate production and intracellular ATP levels (Supplementary Figs. 7b-7c, respectively). Fig. 8k shows results using samples from a representative B-ALL patient with decreased cell viability and proliferation upon Physcion treatment. Similar results were obtained using S3 (Fig. 8g, *right*; Supplementary Figs. 7d-7f). In contrast, Physcion or S3 treatment did not affect cell viability of mononucleocytes in peripheral blood samples or CD34+ progenitors isolated from bone marrow samples from healthy donors (Fig. 8l and Supplementary Figs. 7g-7h), suggesting promising anti-cancer potential of Physcion and S3 without obvious toxicity to human blood cells.

DISCUSSION

Our findings suggest that 6PGD is commonly important for cell proliferation and tumor growth; 6PGD coordinates anabolic biosynthesis and redox homeostasis, at least in part by controlling the intracellular levels of its products Ru-5-P and NADPH (Supplementary Fig. 8a). In a related study, we demonstrated that upregulation of 6PGD by lysine acetylation in cancer cells is common and important for cell proliferation and tumor growth [37]. Thus, in cancer cells, lysine acetylation enhances 6PGD activity [37] to promote oxidative PPP and nucleotide or RNA biosynthesis and keep intracellular Ru-5-P at a physiological level that is sufficient to inhibit LKB1-AMPK signaling, which in turn relieves AMPK-dependent inhibition of ACC1, permitting high levels of lipid biosynthesis to fulfill the request of rapidly growing tumors (Supplementary Fig. 8a, *left*). Attenuation of 6PGD results in decreased Ru-5-P to levels below the physiological concentrations, which in turn not only attenuate nucleotide biosynthesis but also relieve the inhibition of LKB1, leading to activation of AMPK and subsequent inhibition of ACC1 and lipogenesis (Supplementary

Author Manuscript Author Manuscript Author Manuscript Author Manuscript

Fig. 8a, *right*). Our results suggest that 6PGD provides an additional link between oxidative PPP and lipogenesis through Ru-5-P-dependent inhibition of LKB1-AMPK signaling by disrupting active LKB1-MO25-STRAD complex. Although the intracellular level of Ru-5-P decreased in 6PGD knockdown cells, which suggests an important role for 6PGD in maintaining the intracellular Ru-5-P level that cannot be compensated by other pathways, this does not exclude the potential contribution of non-oxidative PPP in maintaining physiological Ru-5-P levels to regulate lipogenesis. In addition, our findings regarding a commonly important role of 6PGD in oxidative PPP in cancer cells are different from the previous report using H1975 lung cancer cells [19, 20], suggesting that 6PGD functions may vary in cancer cells due to different cell types or oncogenic background.

A remaining question is whether the key enzymes along the oxidative PPP including G6PD, gluconolactonase (6-phosphogluconolactonase a.k.a. H6PD) and 6PGD participate in LKB1 regulation using a similar mechanism. Interestingly, we found that knockdown of H6PD essentially reconstitute the phenotypes in cells with 6PGD knockdown, including decreased Ru-5-P levels, increased AMPK activation and reduced cell proliferation (Supplementary Fig. 8b). In contrast, although knockdown of G6PD similarly resulted in decreased Ru-5-P levels, loss of G6PD did not affect AMPK activation nor attenuate cell proliferation (Supplementary Fig. 8c). These results suggest that H6PD and 6PGD probably function in a linear fashion to regulate Ru-5-P levels and consequently AMPK activation and cell proliferation, whereas the role of G6PD in cells is probably much more complicated. G6PD seems dispensable for cell proliferation, suggesting that G6PD knockdown cells may signal through alternative networks via unknown mechanisms to diminish AMPK activation and maintain their proliferative potential. Further studies are warranted to decipher the role of distinct enzymes in the oxidative PPP in cancer cell metabolism and cell proliferation.

We observed that 6PGD inhibitors were more potent to inhibit cell proliferation than 6PGD enzyme activity. This may suggest that 6PGD activity is likely not linearly correlate with cell proliferative potential. Cancer cells might require a certain level of cellular 6PGD activity to maintain cell metabolism and subsequently proliferation. Once 6PGD activity drops below such a threshold (e.g. treatment with 6PGD inhibitor), cancer cells may shut down all the related functions, leading to decreased cell proliferation. Moreover, suppression of 6PGD in A549 cells resulted in reduced cell proliferation with unaltered AMPK phosphorylation and lipogenesis but decreased Ru-5-P and increased ROS, suggesting that such LKB1-deficient cells may still rely on 6PGD-dependent regulation of oxidative PPP flux and subsequent nucleotide biosynthesis and redox homeostasis. The extent of this reliance would determine the responsiveness and sensitivity of LKB1-deficient cells to treatment with 6PGD inhibitors. Additionally, although 6PGD-dependent regulation of the LKB1-AMPK cascade and subsequent lipogenesis through Ru-5-P exists in normal proliferating HaCaT and HFF cells, suppression of 6PGD in these cells does not significantly affect their proliferative potential. These findings provide mechanistic insight into the selective toxicity of 6PGD inhibitors to cancer cells. These translational studies together provide “proof of principle” to suggest anti-6PGD as a promising therapy in clinical treatment of human cancers with commonly elevated 6PGD activity and lysine acetylation [37].

Author Manuscript Author Manuscript Author Manuscript Author Manuscript

Supplementary Material

Refer to Web version on PubMed Central for supplementary material.

ACKNOWLEDGEMENTS

This work was supported in part by NIH grants CA140515, CA183594, CA174786 (J.C.), CA175316 (S.K.), GM071440 (C.H.) and the Pharmacological Sciences Training Grant T32 GM008602 (S.E.), DoD grant W81XWH-12-1-0217 (J.C.), National Natural Science Funds of China No.20902013 (L.Z.), Charles Harris Run For Leukemia, Inc. (H.J.K.) and the Hematology Tissue Bank of the Emory University School of Medicine and the Georgia Cancer Coalition (H.J.K.). J.X., M.T. and T.-L.G. are employees of Cell Signaling Technology, Inc. T.H. is a Fellow Scholar of the American Society of Hematology. S.E. is a NIH pre-doctoral fellow and an ARCS Foundation Scholar. H.J.K., F.R.K., S.K. and J.C. are Georgia Cancer Coalition Distinguished Cancer Scholars. S. K. is a Robbins Scholar. S.K. and J.C. are American Cancer Society Basic Research Scholars. J.C. is a Scholar of the Leukemia and Lymphoma Society.

References

1. Warburg O. On the origin of cancer cells. Science. Science. Science. Science. Science. 1956; 123:309–314. [PubMed: 13298683]
2. Cairns RA, Harris IS, Mak TW. Regulation of cancer cell metabolism. Nature reviews. Cancer. 2011; 11:85–95. [PubMed: 21258394]
3. Kroemer G, Pouyssegur J. Tumor cell metabolism: cancer's Achilles' heel. Cancer Cell. 2008; 13:472–482. [PubMed: 18538731]
4. Christofk HR, et al. The M2 splice isoform of pyruvate kinase is important for cancer metabolism and tumour growth. Nature. 2008; 452:230–233. [PubMed: 18337823]
5. Hitosugi T, et al. Phosphoglycerate mutase 1 coordinates glycolysis and biosynthesis to promote tumor growth. Cancer Cell. 2012; 22:585–600. [PubMed: 23153533]
6. Locasale JW, et al. Phosphoglycerate dehydrogenase diverts glycolytic flux and contributes to oncogenesis. Nature genetics. 2011; 43:869–874. [PubMed: 21804546]
7. Possemato R, et al. Functional genomics reveal that the serine synthesis pathway is essential in breast cancer. Nature. 2011; 476:346–350. [PubMed: 21760589]
8. Vander Heiden MG, et al. Evidence for an alternative glycolytic pathway in rapidly proliferating cells. Science. 2010; 329:1492–1499. [PubMed: 20847263]
9. Tian WN, et al. Importance of glucose-6-phosphate dehydrogenase activity for cell growth. J Biol Chem. 1998; 273:10609–10617. [PubMed: 9553122]
10. Farquharson C, Milne J, Loveridge N. Mitogenic action of insulin-like growth factor-I on human osteosarcoma MG-63 cells and rat osteoblasts maintained in situ: the role of glucose-6-phosphate dehydrogenase. Bone Miner. 1993; 22:105–115. [PubMed: 8251763]
11. Tian WN, et al. Importance of glucose-6-phosphate dehydrogenase activity in cell death. Am J Physiol. 1999; 276:C1121–1131. [PubMed: 10329961]
12. Li D, et al. A new G6PD knockdown tumor-cell line with reduced proliferation and increased susceptibility to oxidative stress. Cancer Biother Radiopharm. 2009; 24:81–90. [PubMed: 19243250]
13. Schafer ZT, et al. Antioxidant and oncogene rescue of metabolic defects caused by loss of matrix attachment. Nature. 2009; 461:109–113. [PubMed: 19693011]
14. Budihardjo II, et al. 6-Aminonicotinamide sensitizes human tumor cell lines to cisplatin. Clinical cancer research : an official journal of the American Association for Cancer Research. 1998; 4:117–130. [PubMed: 9516960]
15. Bravard A, Luccioni C, Muleris M, Lefrancois D, Dutrillaux B. Relationships between UMPK and PGD activities and deletions of chromosome 1p in colorectal cancers. Cancer genetics and cytogenetics. 1991; 56:45–56. [PubMed: 1660788]
16. Jonas SK, et al. Increased activity of 6-phosphogluconate dehydrogenase and glucose-6-phosphate dehydrogenase in purified cell suspensions and single cells from the uterine cervix in cervical intraepithelial neoplasia. British journal of cancer. 1992; 66:185–191. [PubMed: 1637668]

Author Manuscript Author Manuscript Author Manuscript Author Manuscript

17. Basu J, et al. Alterations in erythrocyte glutathione metabolism associated with cervical dysplasias and carcinoma in situ. Cancer investigation. 1993; 11:652–659. [PubMed: 8221197]
18. Giusti L, et al. Fine-needle aspiration of thyroid nodules: proteomic analysis to identify cancer biomarkers. J Proteome Res. 2008; 7:4079–4088. [PubMed: 18665625]
19. Sukhatme VP, Chan B. Glycolytic cancer cells lacking 6-phosphogluconate dehydrogenase metabolize glucose to induce senescence. FEBS letters. 2012; 586:2389–2395. [PubMed: 22677172]
20. Chan B, VanderLaan PA, Sukhatme VP. 6-Phosphogluconate dehydrogenase regulates tumor cell migration in vitro by regulating receptor tyrosine kinase c-Met. Biochem Biophys Res Commun. 2013; 439:247–251. [PubMed: 23973484]
21. Shaw RJ, et al. The tumor suppressor LKB1 kinase directly activates AMP-activated kinase and regulates apoptosis in response to energy stress. Proceedings of the National Academy of Sciences of the United States of America. 2004; 101:3329–3335. [PubMed: 14985505]
22. Woods A, et al. LKB1 is the upstream kinase in the AMP-activated protein kinase cascade. Current biology : CB. 2003; 13:2004–2008. [PubMed: 14614828]
23. Shackelford DB, Shaw RJ. The LKB1-AMPK pathway: metabolism and growth control in tumour suppression. Nature reviews. Cancer. 2009; 9:563–575.
24. Park SH, et al. Phosphorylation-activity relationships of AMPK and acetyl-CoA carboxylase in muscle. Journal of Applied Physiology. 2002; 92:2475–2482. [PubMed: 12015362]
25. Hardie DG. Regulation of Fatty-Acid and Cholesterol-Metabolism by the Amp-Activated Protein-Kinase. Biochimica Et Biophysica Acta. 1992; 1123:231–238. [PubMed: 1536860]
26. Jeon SM, Chandel NS, Hay N. AMPK regulates NADPH homeostasis to promote tumour cell survival during energy stress. Nature. 2012; 485:661–665. [PubMed: 22660331]
27. Fullerton MD, et al. Single phosphorylation sites in Acc1 and Acc2 regulate lipid homeostasis and the insulin-sensitizing effects of metformin. Nature medicine. 2013; 19:1649–1654.
28. Sommercorn J, Freedland RA. Regulation of hepatic phosphofructokinase by 6-phosphogluconate. J Biol Chem. 1982; 257:9424–9428. [PubMed: 6213607]
29. Davies SP, Sim AT, Hardie DG. Location and function of three sites phosphorylated on rat acetyl-CoA carboxylase by the AMP-activated protein kinase. European journal of biochemistry / FEBS. 1990; 187:183–190. [PubMed: 1967580]
30. Ha J, Daniel S, Broyles SS, Kim KH. Critical phosphorylation sites for acetyl-CoA carboxylase activity. J Biol Chem. 1994; 269:22162–22168. [PubMed: 7915280]
31. Kudo N, Barr AJ, Barr RL, Desai S, Lopaschuk GD. High rates of fatty acid oxidation during reperfusion of ischemic hearts are associated with a decrease in malonyl-CoA levels due to an increase in 5'-AMP-activated protein kinase inhibition of acetyl-CoA carboxylase. J Biol Chem. 1995; 270:17513–17520. [PubMed: 7615556]
32. Munday MR, Campbell DG, Carling D, Hardie DG. Identification by amino acid sequencing of three major regulatory phosphorylation sites on rat acetyl-CoA carboxylase. European journal of biochemistry / FEBS. 1988; 175:331–338. [PubMed: 2900138]
33. Mihaylova MM, Shaw RJ. The AMPK signalling pathway coordinates cell growth, autophagy and metabolism. Nature cell biology. 2011; 13:1016–1023. [PubMed: 21892142]
34. Boudeau J, et al. MO25alpha/beta interact with STRADalpha/beta enhancing their ability to bind, activate and localize LKB1 in the cytoplasm. The EMBO journal. 2003; 22:5102–5114. [PubMed: 14517248]
35. Zeqiraj E, Filippi BM, Deak M, Alessi DR, van Aalten DM. Structure of the LKB1-STRAD-MO25 complex reveals an allosteric mechanism of kinase activation. Science. 2009; 326:1707–1711. [PubMed: 19892943]
36. Marignani PA, et al. Novel splice isoforms of STRADalpha differentially affect LKB1 activity, complex assembly and subcellular localization. Cancer biology & therapy. 2007; 6:1627–1631. [PubMed: 17921699]
37. Shan C, et al. Lysine acetylation activates 6-phosphogluconate dehydrogenase to promote tumor growth. Molecular cell. 2014; 55:552–565. [PubMed: 25042803]

Author Manuscript Author Manuscript Author Manuscript Author Manuscript

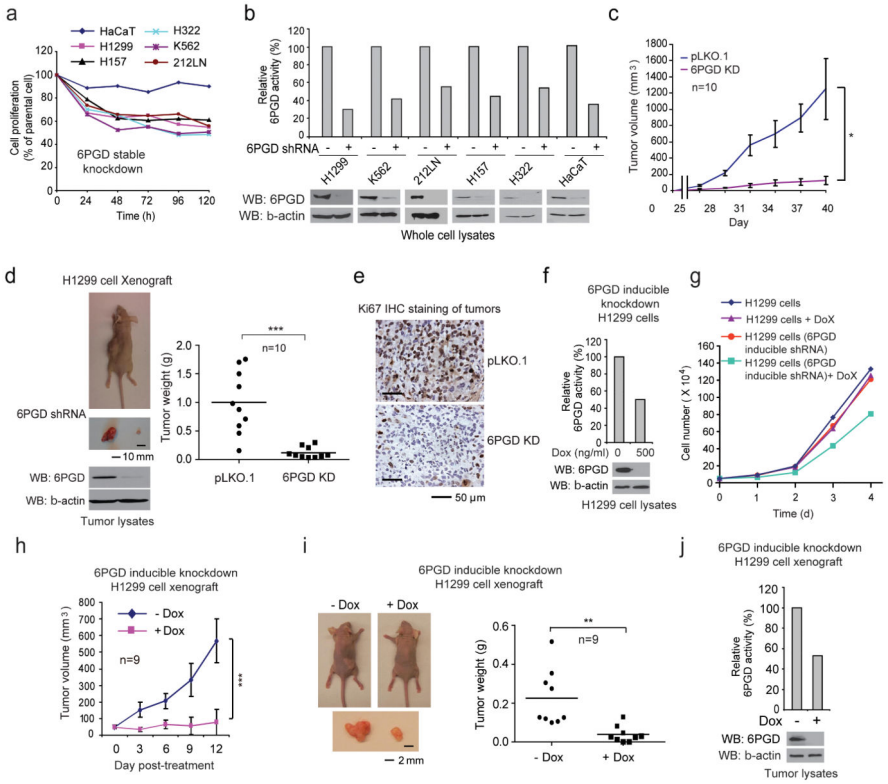

Fig. 1.

6PGD is important for cancer cell proliferation and tumor growth. (**a-b**) Cell proliferation rates determined by cell counting (a) and 6PGD activity (b; *upper*) in diverse human cancer cells with 6PGD stable knockdown (b; *lower*), which were normalized to the corresponding control vector cells. Keratinocyte HaCaT cells were included as controls. (**c**) Tumor growth was compared between xenograft nude mice injected with 6PGD KD H1299 cells and control vector cells. (**d**) *Left*: Dissected tumors in a representative nude mouse are shown. Scale bar represents 10 mm. *Right:* Tumor mass in xenograft nude mice injected with 6PGD KD H1299 cells compared to mice injected with the control vector cells. (**e**) Representative images of IHC staining of Ki-67 from xenograft mice injected with control vector or 6PGD KD H1299 cells. Scale bars indicate 50 μM. (**f**) 6PGD activity (*upper*) and protein expression (*lower*) in H1299 cells with inducible knockdown of 6PGD in the presence and absence of doxycycline (Dox). (**g**) Cell proliferation rates determined by cell counting in H1299 cells with inducible 6PGD knockdown and control cells in the presence and absence of Dox. (**h**) Tumor growth was compared between xenograft mice injected with H1299 cells with inducible 6PGD knockdown fed with drinking water in the presence or absence of Dox. (**i-j**) Dissected tumors in two representative nude mice (i; *left*) and tumor mass of xenograft mice injected with H1299 cells with inducible 6PGD knockdown (i; *right*) fed with drinking water in the presence or absence of Dox are shown. Scale bars represent 2 mm. 6PGD activity (*upper*) and protein expression (*lower*) in tumor lysates are shown (j). (a-g, and j) Data are from a single experiment that is representative of 2 independent experiments for (a) and 3 independent experiments for (b-g, and j). Source data for independently repeated experiments are provided in Supplementary Table 1. (c) Mean ± S.E.M.; n=10 tumors from

Author Manuscript Author Manuscript Author Manuscript Author Manuscript

10 mice, (d) n=10 tumors from 10 mice; centerlines represent means, (h) Mean ± S.E.M.; n=9 tumors from 9 mice, (i) n=9 tumors from 9 mice; centerlines represent means. The P values were determined by two-sided unpaired Student's *t*-test for (c, h, and i) and paired two-sided Student's *t*-test for (d) (*: $0.01<p<0.05$; **: $0.001<p<0.01$; ***: $p<0.001$). (a-g, j). Source data for independent replications and experiments with sample size<5 are available in Supplementary Table 1. Uncropped Western blots are provided in Supplementary Figure 9.

Author Manuscript Author Manuscript Author Manuscript Author Manuscript

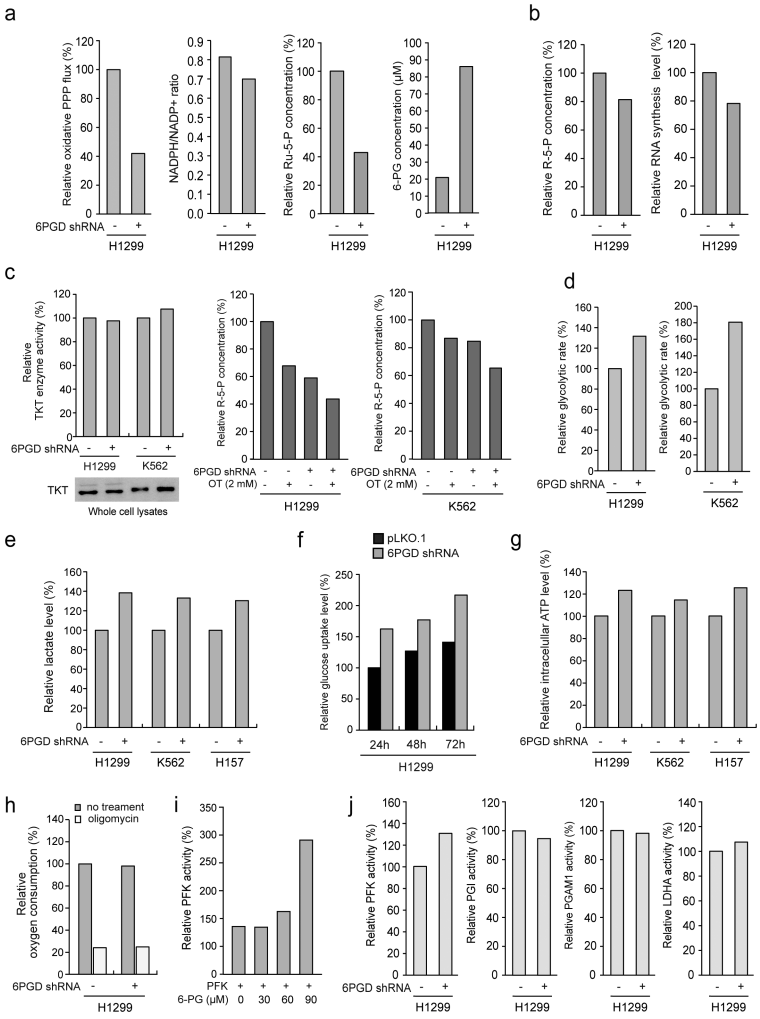

Fig. 2.

6PGD contributes to regulation of oxidative PPP and glycolysis. (**a**) 6PGD KD and control cells harboring an empty vector were tested for oxidative PPP flux and NADPH/NADP$^+$ ratio (*left panels*), and intracellular levels of Ru-5-P and 6-PG (*right panels*). (**b**) 6PGD KD H1299 cells and control vector cells were tested for intracellular R-5-P levels (b; *left*) and RNA biosynthesis (b; *right*). (**c**) *Left*: H1299 and K562 cells with stable knockdown of 6PGD were tested for transketolase (TKT) protein expression (*lower*) and enzyme activity (*upper*) levels. *Right*: H1299 and K562 cells with stable knockdown of 6PGD were tested for intracellular R-5-P levels in the presence and absence of TKT inhibitor oxythiamine (OT). (**d-g**) 6PGD KD and vector control cells were tested for glycolytic rate (d), lactate production (e), glucose uptake rate (f) and intracellular ATP level (g). (**h**) 6PGD KD H1299 cells and control vector cells were tested for oxygen consumption rate in the presence or absence of 100 nM oligomycin (ATP synthase inhibitor). (**i**) H1299 cell lysates were incubated with increasing concentrations of 6-PG, followed by in vitro PFK enzyme activity assay. PFK activities were normalized to the control sample without 6-PG treatment. (**j**) 6PGD KD and control vector H1299 cells were tested for activity of glycolytic enzymes including PFK, PGI, PGAM1 and LDHA. (a-j) Data are from a single experiment that is

Author Manuscript Author Manuscript Author Manuscript Author Manuscript

representative of 2 independent experiments for (a, g; middle, and h-j), 3 independent experiments for (b-d, and f), and 4 independent experiments for (e and g; left and right). Source data for independent replications and experiments with sample size<5 are available in Supplementary Table 1. Uncropped Western blots are provided in Supplementary Figure 9.

Author Manuscript Author Manuscript Author Manuscript Author Manuscript

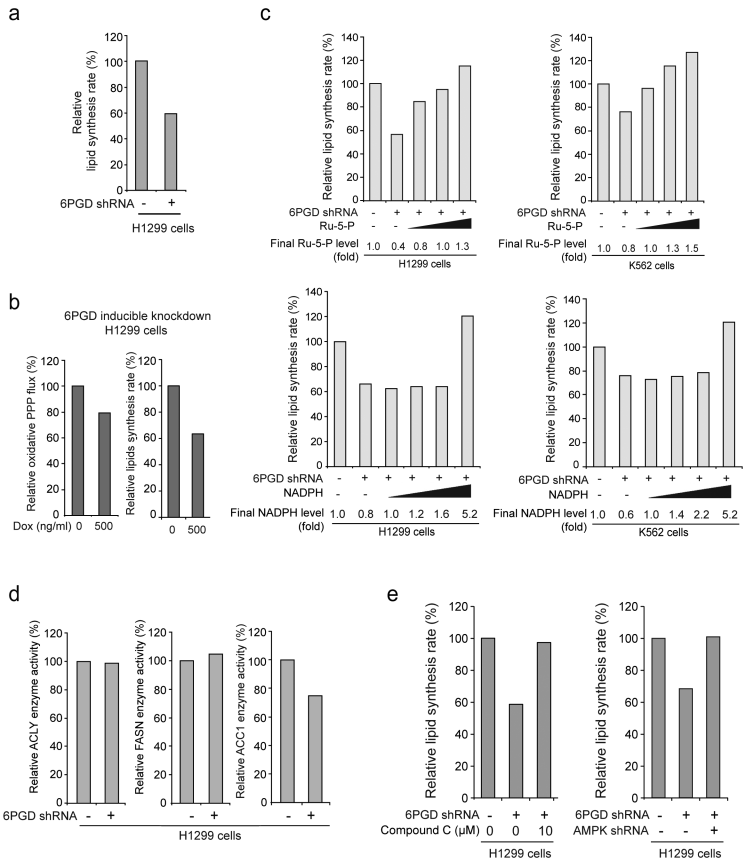

Fig. 3.

6PGD contributes to lipogenesis through regulation of AMPK and ACC1 activity. (**a**) 6PGD KD and control cells harboring an empty vector were tested for lipogenesis. (**b**) H1299 cells with inducible knockdown of 6PGD were tested for oxidative PPP flux (*left*) and lipogenesis (*right*) in the presence and absence of Dox. (**c**) Cell lysates from 6PGD KD H1299 and K562 cells were treated with increasing concentrations of Ru-5-P (*upper* panels) or NADPH (*lower* panels) for 12 hours, followed by lipid biosynthesis assay. Final levels (fold) of Ru-5-P and NADPH were normalized to the control vector cells without treatment with Ru-5-P or NADPH, respectively. Lipid biosynthesis rates (%) were normalized to the control vector cells without treatment with Ru-5-P (*upper*) or NADPH (*lower*). (**d**) 6PGD KD cells and control vector H1299 cells were tested for enzyme activity of ACLY (*left*), FASN (*middle*) and ACC1 (*right*). Enzyme activities were normalized to the control vector cells. (**e**) Cell lysates from 6PGD KD H1299 cells were treated with or without AMPK inhibitor Compound C (10 μM) for 12 hours (*left*) and 6PGD stable KD cells were infected with lentivirus harboring AMPK shRNA (*right*). The samples were applied to lipid biosynthesis assay. (a-e) Data are from a single experiment that is representative of 3 independent experiments for (a and c) and 2 independent experiments for (b and d-e). Source data for independent replications and experiments with sample size<5 are available in Supplementary Table 1. Uncropped Western blots are provided in Supplementary Figure 9.

Author Manuscript Author Manuscript Author Manuscript Author Manuscript

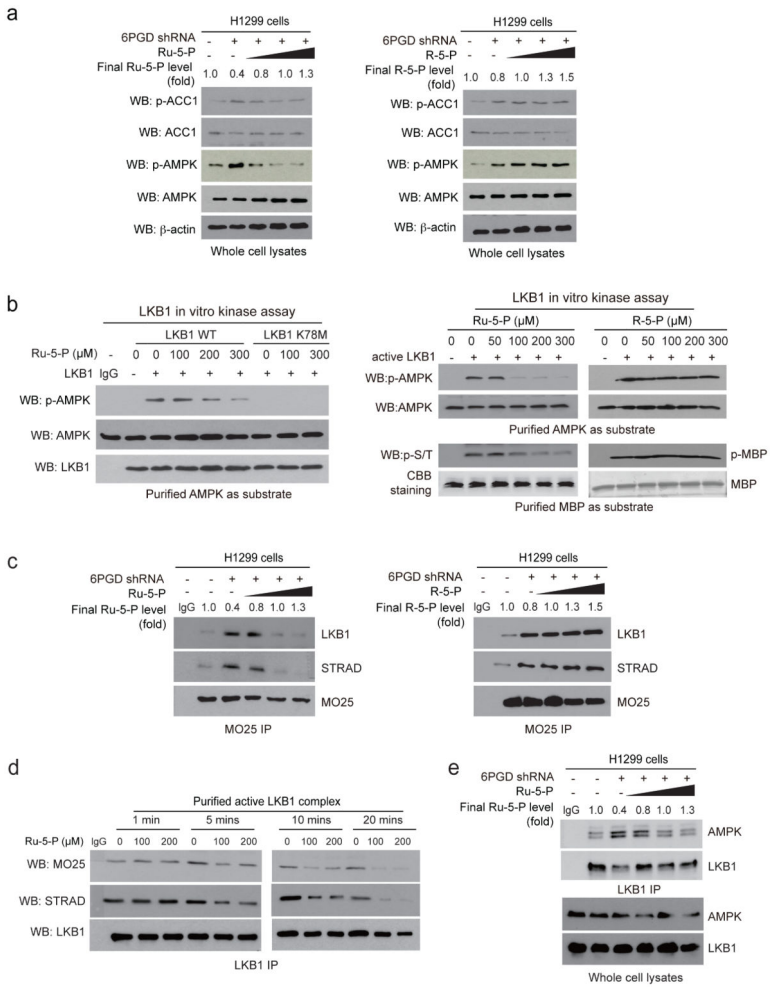

Fig. 4.

Ru-5-P inhibits LKB-AMPK pathway by disrupting active LKB1 complex. (a) Cell lysates from 6PGD KD H1299 cells were treated with increasing concentrations of Ru-5-P (*left*) or R-5-P (*right*) for 4 hours, followed by Western blot for phosphorylation levels of AMPK (pT172) and ACC1 (pS79). Final levels (fold) of Ru-5-P or R-5-P were normalized to the control vector cells without treatment. (b) *In vitro* LKB1 kinase assays were performed using LKB1 wild type (WT) or a kinase dead form (K78M) purified from A549 cells (*left panel*) or LKB1 WT purified from H1299 cells (*right panel*) incubated with recombinant AMPK (*left* and *upper right*) or MBP (*lower right*) as substrates in the presence of increasing concentrations of Ru-5-P (*left*), or Ru-5-P or R-5-P (*right*) at 37 °C for 20 minutes. Samples were applied for Western blot. (c) Cell lysates of 6PGD KD H1299 cells were incubated with increasing concentrations of Ru-5-P (*left*) or R-5-P (*right*), followed by immunoprecipitation of MO25 and Western blot to detect co-immunoprecipiated LKB1 and STRAD. (d) Purified active LKB1 complex purchased from Upstate (Millipore) were incubated with Ru-5-P (100 or 200 μM) for indicated time points, followed by immunoprecipitation of LKB1 and Western blot to detect co-immunoprecipiated MO25. (e) Cell lysates of 6PGD KD H1299 cells were incubated with increasing concentrations of Ru-5-P, followed by immunoprecipitation of LKB1 and Western blot to detect co-

Author Manuscript Author Manuscript Author Manuscript Author Manuscript

immunoprecipiated AMPK. (a-e) Results of one representative experiment from at 2 independent experiments (a-b) and 3 independent experiments (c-e) are shown. Uncropped Western blots are provided in supplementary Figure 9.

Author Manuscript Author Manuscript Author Manuscript Author Manuscript

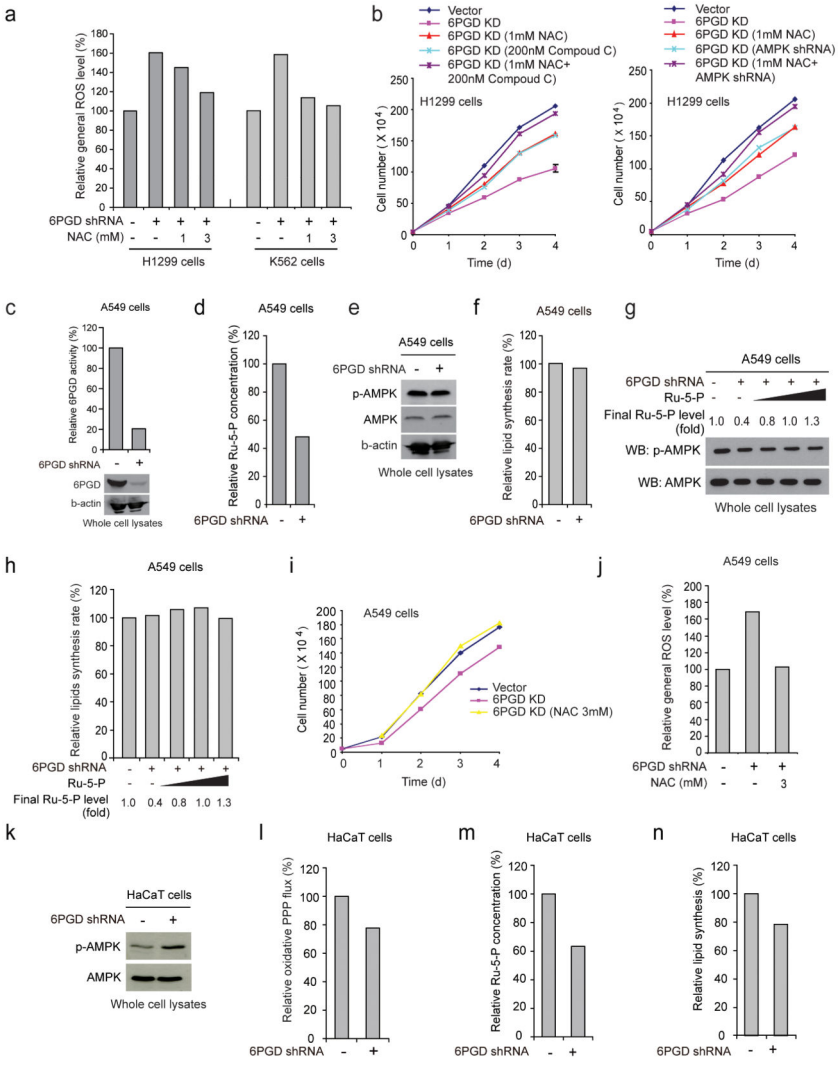

Fig. 5.

6PGD controls Ru-5-P level to regulate LKB1-AMPK signaling and subsequently ACC1 activity and lipogenesis. (**a**) 6PGD KD H1299 (*left*) and K562 (*right*) cells were assayed for general ROS levels in the absence and presence of NAC (1 and 3 mM) by measuring intracellular ROS-mediated DCFDA oxidation to fluorescent DCF by flow cytometry. The relative general ROS levels were normalized to the control vector cells without NAC treatment. (**b**) Cell proliferation rates were determined by cell counting in 6PGD KD H1299 cells treated with either or both NAC and Compound C (*left*) or 6PGD KD cells treated with either or both AMPK shRNA and NAC (*right*). (**c-f**) LKB1-deficient A549 cells with 6PGD knockdown (c) and control vector cells were assayed for intracellular Ru-5-P levels (d), phosphorylation levels of AMPK (e), and lipogenesis (f). (**g-h**) Cell lysates from 6PGD KD A549 cells were treated with increasing concentrations of Ru-5-P, followed by Western blot for phosphorylation levels of AMPK (g) or lipogenesis assay (h). Final levels (fold) of Ru-5-P were normalized to the control vector cells without treatment. (**i-j**) A549 vector and 6PGD knockdown cells were tested for cell proliferation rate by cell counting (i) and ROS level (j) in the presence or absence of NAC (3 mM). (**k-n**) Normal proliferating HaCaT vector and

Author Manuscript Author Manuscript Author Manuscript Author Manuscript

6PGD knockdown cells were assayed for phosphorylation levels of AMPK (k), oxidative PPP flux rate (l), intracellular Ru-5-P levels (m), and lipogenesis (n). (a-n) Data are from a single experiment that is representative of 3 independent experiments for (a, c, e, g) and 2 independent experiments for (b, d, f, h-n). Source data for independent replications and experiments with sample size<5 are available in Supplementary Table 1. Uncropped Western blots are provided in Supplementary Figure 9.

Author Manuscript Author Manuscript Author Manuscript Author Manuscript

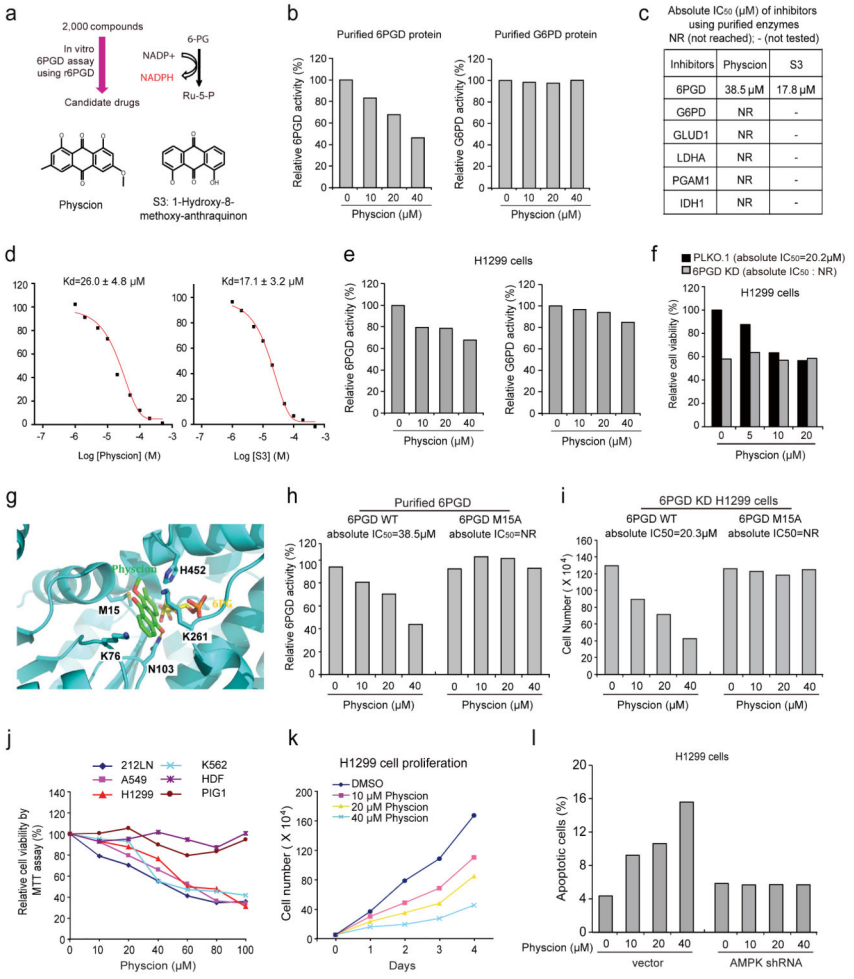

Fig. 6.

Identification of Physcion and its derivative S3 as 6PGD inhibitors (**a**) *Upper*: Screening strategy for lead compounds as 6PGD inhibitors. *Lower*: Structure of Physcion and its derivative S3. (**b**) Purified 6PGD (*left*) and G6PD (*right*) were assayed for 6PGD and G6PD activity, respectively, in the presence of Physcion. (**c**) Absolute IC_{50} values of Physcion and S3 were determined in activity assays using purified enzymes. (**d**) Kd values were determined for Physcion or S3 binding to purified human 6PGD proteins. The fluorescence intensity (Ex: 280nm, Em: 350nm) was measured [37]. (**e-f**) Physcion-treated H1299 cells were assayed for 6PGD (e; *left*) and G6PD (e; *right*) activity, and cell viability (f). (**g**) Schematic representation of molecular docking study of Physcion based on the crystal structure of 6PGD (PDB code: 3FWN) in complex with its substrate 6-PG. Physcion (green) is docked in a pocket near the binding site of 6-PG (yellow) that is surrounded by residues including M15, K76, K261 and H452. (**h**) Purified 6PGD WT (*left*) and M15A mutant (*right*) were treated with Physcion and assayed for 6PGD activity. Absolute IC_{50} values are shown; NR=not reached. (**i**) H1299 6PGD knockdown cells were transfected with 6PGD WT (*left*) and M15A mutant (*right*), followed by cell proliferation assay based on cell numbers in the presence of Physcion. (**j**) Cell viability of Physcion-treated human cancer cells were determined by MTT assay. Normal proliferating human dermal fibroblasts (HDF)

Author Manuscript Author Manuscript Author Manuscript Author Manuscript

and melanocyte PIG1 cells were included as controls. (**k**) Cell proliferation rates of H1299 cells treated with Physcion were determined. (**l**) Apoptotic cell death (48 hours) of H1299 cells harboring AMPK shRNA or an empty vector in the presence of Physcion were determined by annexin V staining. Data are from a single experiment that is representative of 3 independent experiments for (b, e, h), 2 independent experiments for (f, i, l), and 4 independent experiments for (j-k). Source data for independent replications and experiments with sample size<5 are available in Supplementary Table 1. Uncropped Western blots are provided in Supplementary Figure 9.

Author Manuscript Author Manuscript Author Manuscript Author Manuscript

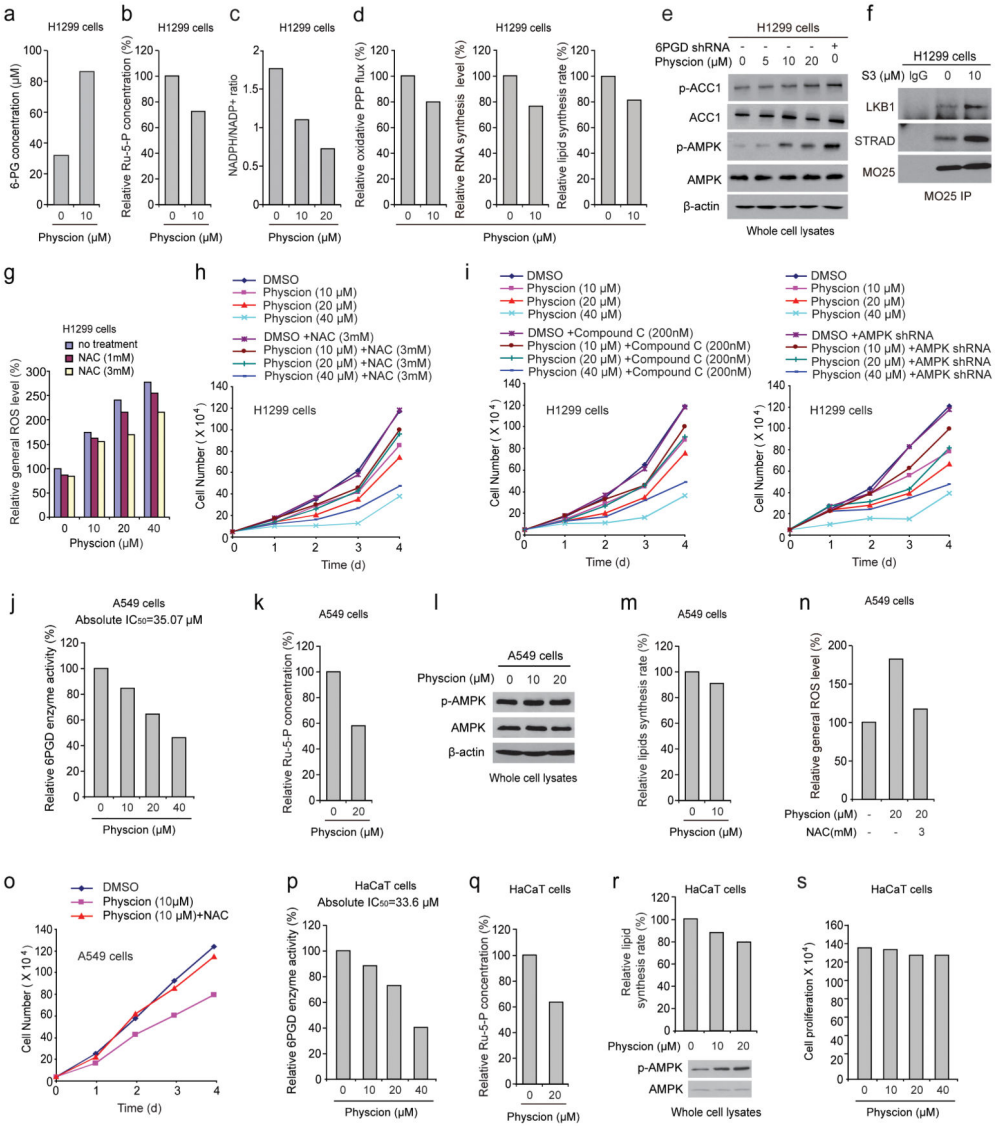

Fig. 7.

6PGD inhibitor Physcion inhibits cancer cell metabolism and proliferation. (**a-d**) H1299 cells were assayed for intracellular concentration of 6-PG (a) and Ru-5-P (b), NADPH/NADP$^+$ ratio (c), as well as oxidative PPP flux and biosynthesis of RNA and lipids (d) in the presence and absence of Physcion. (**e**) H1299 cells were treated with increasing concentrations of Physcion, followed by Western blot to detect phosphorylation levels of ACC1 (pS79; *upper*) and AMPK (pT172; *lower*). 6PGD KD cells were included as a control. (**f**) Cell lysates of S3-treated H1299 cells were used for immunoprecipitation of MO25 and Western blot to detect co-immunoprecipiated LKB1 and STRAD. (**g-h**) H1299 cells treated with or without Physcion were assayed for general ROS levels (g) and cell proliferation rates by cell counting (h) in the presence and absence of NAC. (**i**) H1299 cells treated with or without Physcion were assayed for cell proliferation rates by cell counting in the presence and absence of Compound C (*left*) or lentivirus harboring AMPK shRNA (*right*). (**j-o**) Effects of treatment with Physcion on LKB1-deficient A549 cells were assayed

Author Manuscript Author Manuscript Author Manuscript Author Manuscript

for 6PGD activity (j), intracellular Ru-5-P levels (k), phosphorylation levels of AMPK (l) and lipid biosynthesis (m), as well as general ROS levels (n) and cell proliferation rates by cell counting (o) in the presence and absence of NAC. (**p-s**) Effects of Physcion treatment on normal proliferating HaCaT cells were assayed for 6PGD activity (p), intracellular Ru-5-P levels (q), phosphorylation levels of AMPK and lipid biosynthesis (r), as well as cell proliferation rates by cell counting (s). (a-s) Data are from a single experiment that is representative of 3 independent experiments for (b-c, e) and 2 independent experiments for (a, d, f-s). Source data for independent replications and experiments with sample size<5 are available in Supplementary Table 1. Uncropped Western blots are provided in Supplementary Figure 9.

Author Manuscript Author Manuscript Author Manuscript Author Manuscript

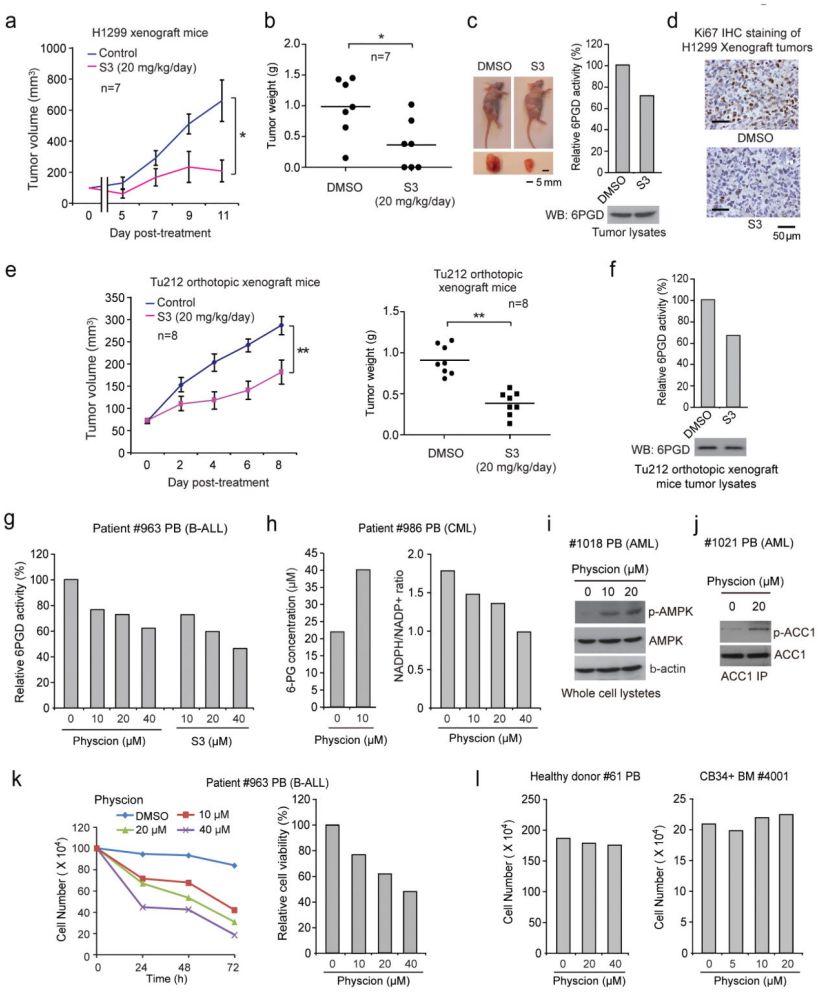

Fig. 8.

6PGD inhibitors effectively attenuate tumor growth in xenograft mice and cell proliferation of human primary leukemia cells. (a-b) Tumor growth curve (a) and tumor mass (b) in H1299-xenograft mice treated with S3 or DMSO. (c) *Left*: Dissected tumors in representative mice treated with DMSO or S3 are shown. Scale bar represents 5 mm. *Right*: 6PGD enzyme activity in tumor lysates of H1299 xenograft mice treated with DMSO or S3 is shown. (d) Representative images of IHC staining of Ki-67 from H1299 xenograft mice treated with DMSO or S3 are shown. Scale bars indicate 50 μM. (e-f) Tumor growth curve (e; *left*) and tumor mass (e: *right*) in orthotopic xenograft nude mice injected with Tu212 cells treated with S3 or DMSO. 6PGD activity (*upper*) and protein (*lower*) levels in tumor lysates are shown (f). (g) 6PGD activity in Physcion- or S3-treated human primary leukemia cells isolated from PB samples from a representative B-ALL patient. (h) 6-PG levels (*left*) and NADPH/NADP$^+$ ratio (*right*) in Physcion-treated human primary leukemia cells from a representative CML patient. (i-j) AMPK (pT172; i) and ACC1 (pS79; j) phosphorylation levels were examined by immunoblotting using Physcion-treated human primary leukemia cells isolated from PB samples from representative AML patients. (k) Cell proliferation (*left*) and viability (*right*) in Physcion-treated human primary leukemia cells isolated from PB samples from a representative B-ALL patient. (l) Physcion shows no toxicity in

Author Manuscript Author Manuscript Author Manuscript Author Manuscript

treatment (72h) of peripheral blood cells (*left*) and $CD34^+$ cells isolated from bone marrow samples (*right*) from representative healthy human donors. PB: peripheral blood; BM: bone marrow; B-ALL: Acute B Lymphoblastic Leukemia; AML: Acute Myeloid Leukemia. (a) Mean ± S.E.M.; n=7 tumors from 7 mice, (b) n=7 tumors from 7 mice; centerlines represent means, (e) Mean ± S.E.M.; n=8 tumors from 8 mice; centerlines represent means. The P values were determined by two-sided unpaired Student's *t*-test for (b and e) (ns: not significant; *: $0.01<p<0.05$; **: $0.001<p<0.01$) (a-c, f) Data are from a single experiment that is representative of 2 independent experiments. Source data for independent replications and experiments with sample size<5 are available in Supplementary Table 1. Uncropped Western blots are provided in Supplementary Figure 9.